International Journal of Multiphysics
Volume 18, No. 3, 2024
ISSN: 1750-9548

Assessment of International Seismic Design Codes for Partially Filled Elevated Water Tanks Using Experimental and Numerical Investigations

Atef Eraky [1], Khaled Essam [1], Abdallah Salama [1]

[1]Department of Structural Engineering, Zagazig University, Egypt
∗Corresponding author, E-mail: AEAmien@eng.zu.edu.eg, khaledissam2016@gmail.com

Abstract

Elevated water tanks (EWTs) are one of the most important structures, particularly in highly seismic regions, due to their role in supplying water and extinguishing fires during and after an earthquake. Therefore, they should be designed to withstand the expected seismic loads. This paper aims to evaluate current Response Spectrum Analysis used in Eurocode 8, ACI 350.3-06, and ASCE 7-16 for EWTs. These codes are based on the simplified theory expressed by the method of mass-spring equivalent system. In this study, finite element models of the EWT based on different soil types, medium and hard soil at various levels of tank fullness, are analyzed using ANSYS Software, considering the water sloshing effect to evaluate the code provisions of EWTs, A comprehensive time history analysis is performed under seismic loading. To provide a more accurate assessment of the EWT frequencies, a laboratory experiment using Digital Image Correlation (DIC) was conducted. The maximum shear force and bending moment at the tank's base are analyzed under several scenarios. The results indicated that current international may not provide precise seismic response predictions for EWTs, especially under variable fill conditions, and that the sloshing phenomenon on the water's free surface is a crucial component of tank study and design.

Keywords: Elevated water tanks (EWTs), Fluid structure interaction, Seismic response, DIC.

1. Introduction

Water tanks, especially elevated water tanks (EWTs), are used as storage and supply facilities for both drinking and fire insurance towns usually, on reinforced concrete (R.C.) or steel base, R.C. shaft, or masonry pedestals. Water tanks are provided to obtain high water pressure by gravity before supplying water to cities via the pipeline network. These tanks are also heavy buildings, meaning that a larger portion of their weight is centered on a large height. In high seismic intensity zones, these elevated water tanks are of great importance. The success of these structures during operation and after the earthquake is therefore of crucial concern. Due to the lack of water or the difficulty of extinguishing fires during earthquakes, the collapse of these water tanks can cause severe risks for people.

Many post-earthquake reports on major earthquakes provide information about a large number of water tanks with severe damage Rai [1], Soroushnia et al. [2], so the reliability of these tanks against earthquake load failure is a source of great concern. These structures must also have adequate strength and be free of cracks Seleemah & El-Sharkawy [3], Sezen et al. [4], Chaduvula et al. [5].

Seismic study of elevated tanks is more complicated than other structures owing to water and soil-structure interactions. Several research articles and international seismic codes, such as ACI 371R-08 [6], ACI 350.3-06 [7], Euro code 8 (EC-8) [8], IITK-GSDMA [9] and Egyptian code for loads ECP 201[10] rely on the simplified theory expressed by the method of mass-spring equivalent system Housner [11] with some modifications by other researchers. Younan & Veletsos [12], Anestis S Veletsos & Younan [13] studied the responses to horizontal base shaking for solid-containing cylindrical tanks in case of the wall tank flexibility and rigidity. Haroun & Housner [14] developed a ground-supported tank model which takes into account the flexibility

of the tank walls. Haroun & Ellaithy [15] proposed an equivalent mechanical model for the evaluation of elevated water tanks' dynamic response, and also studied both a cross-braced frame and a concrete pedestal tower. Moslemi et al. [16] assessed of seismic performance of conical elevated tanks using displacement-based fluid elements. El Damatty et al. [17] performed the first experimental study on a small-scale combined liquid-filled conical shell model. To evaluate their dynamic parameters, a shake table test was performed. Dutta et al. [18] studied the seismic behavior of elevated tanks considering soil-structure interaction and presented the design recommendations. Kianoush & Ghaemmaghami [19] concluded that the seismic behavior of the fluid–tank–soil system is highly responsive to the earthquake record's frequency characteristics. Livaoğlu & Doğangün [20] suggested a simple analytical model for the seismic analysis of elevated tank foundation-soil systems, using an added mass approach for the fluid-structure interaction and the massless foundation approaches for the soil-structure interactions. Hussein and Yousef [21] concluded that considering fluid-structure-Soil Interaction increase the fundamental period of vibration and the first free mode shape of vibration is adequate for the analysis of EWTs. Meng et al. [22] concluded that soil stiffness influences the seismic response of liquid storage tanks. Jogi, and Jayalekshmi. [23] assessed of the impact of the SSI on the seismic behaviour of EWT at each different filling condition of container tank. They Conclude that the most critical circumstances are those in which the tank is one third full and when soft soil is the type of ground supporting it. Al-Khafaji et al. [24] performed a seismic analysis on a spherical elevated storage tank under the impact of an earthquake for three different filling ratios of the tank (0.00%, 53.30%, and 71.11% respectively). They concluded that a 53.3% fullness ratio is comparatively more hazardous than a 71.11% ratio, attributing this to the more severe water movement in the former case. Patel and Patel [25] performed a time history analysis on an EWT considering the effect of the water level within the tank and subsoil condition during the seismic analysis. They concluded that responses like base shear, overturning moment, top displacement, and sloshing displacement for half filled condition were higher than both full and empty conditions.

Recent studies have used advanced modeling techniques to assess the seismic response of complex structures, such as coupled tall buildings [26], offering insights applicable to EWTs. To complement these numerical and experimental techniques such as Digital Image Correlation (DIC) have gained prominence in recent years. DIC is a valuable optical technique used to measure deformation, strain, and displacement in structures. Its main advantage is being non-contact, unlike traditional methods like strain gauges or extensometers. This prevents any alteration in the material’s behavior during testing, making it especially suitable for sensitive or fragile specimens. The accuracy of frequency estimation of natural frequency for the EWTs is significantly improved by using digital image correlation (DIC). Combining DIC with structural frequency analysis bridges the gap between theory and experiment, offering deeper insight into tank performance under different loads. Last time, many researchers showed interest in structural monitoring by using this technique (DIC) [27–32].

The filling ratio plays a crucial role in determining the seismic response of EWTs. Unlike conventional structures with constant mass. These facilities are characterized by a variable mass condition due to varying water levels, which significantly influence their dynamic behavior. However, the literature reveals limited research on the seismic performance of EWTs under different fill levels. This work investigates the impact of water sloshing on the seismic response of EWTs at various filling conditions and evaluates the response spectrum method used in the several international codes of practice for seismic analysis of EWTs.

2. Seismic analysis methodology of EWTs

In the literature, there are many simplified procedures to study the seismic behavior of tanks as proposed by Housner (1963)[11], Bauer (1964)[33], and Veletsos et al. [34]. Housner's two-mass equivalent model [11] is prominently featured in numerous international seismic standards and design guidelines for liquid storage tanks [7–9, 35]. Housner introduced a streamlined approach for the seismic response analysis of EWTs using a two-mass spring equivalent system for fixed-base elevated tanks, as illustrated in Figure 1 [11, 20]. Given that typical water tanks have a free water surface, the water inside can slosh during an earthquake, effectively transforming the tank into a two-mass structure. When a liquid-containing tank vibrates, the liquid exerts pressure on the tank walls, which can be characterized by two distinct masses, including impulsive and convective masses. The liquid in the lower portion of the tank vessel acts as a mass rigidly attached to the vessel wall and base, termed the impulsive liquid mass (mi). Conversely, the liquid in the upper region of the tank undergoes sloshing motions and is referred to as the convective liquid mass (mc). The structure mass is also split into two portions. The first part includes the

tank container mass and two-thirds of the staging mass as per ACI 371R [35]. This container mass comprises the weight of the roof slab, container walls, gallery, floor slab, and beams. The residual portion of the staging mass is considered to directly impact the foundation. Epstein [36] further refined Housner's two-mass model, which has subsequently gained widespread acceptance in the seismic design of elevated tanks.

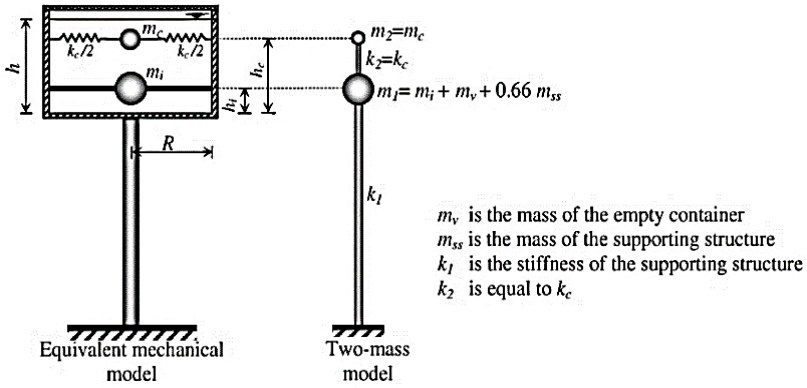

Figure 1 : Two mass model for EWTs suggested by Housner [37].

2.1. Seismic analysis of EWTS according to Eurocode-8

The seismic behavior of the EWTs can be assessed in the Eurocode-8 model using the equations, equivalent masses, and their respective heights from the container base, as detailed in Table 1. In this table, the coefficient C_i is dimensionless, whereas C_c has the units of $(s/m^{1/2})$, m is the total liquid mass, h_i' and h_c' are the heights of the impulsive and convective masses mi and mc, respectively. These parameters are utilized to express the overturning moment below the base plate.

Table 1: Recommended design values for the first impulsive and convective modes of vibration as a function of the tank height-to-radius ratio (h/R) (Eurocode-8, 2006) [8].

H/R	Ci	Cc	mi /m	mc /m	hi/H	hc/H	hi'/H	hc'/H
0.3	9.28	2.09	0.176	0.824	0.400	0.521	2.640	3.414
0.5	7.74	1.74	0.300	0.700	0.400	0.543	1.460	1.517
0.7	6.97	1.60	0.414	0.586	0.401	0.571	1.009	1.011
1.0	6.36	1.52	0.548	0.452	0.419	0.616	0.721	0.785
1.5	6.06	1.48	0.686	0.314	0.439	0.690	0.555	0.734
2.0	6.21	1.48	0.763	0.237	0.448	0.751	0.500	0.764
2.5	6.56	1.48	0.810	0.190	0.452	0.794	0.480	0.796
3.0	7.03	1.48	0.842	0.158	0.453	0.825	0.472	0.825

In Housner's methodologies, the two masses (m_1 and m_2) are considered uncoupled, and seismic forces on the model are approximated by addressing two distinct single-degree-of-freedom systems. By leveraging standard structural dynamic techniques, the two-degree-of-freedom system can be transformed into two separate single-degree-of-freedom systems, as depicted in Figure 2, where, M_1* and M_2*; h_1*and h_2*; k_1*and k_2* are the effective masses, effective heights, and effective stiffnesses of the first and the second modes, respectively. These modal properties can be evaluated using equations (1) and (2) [38].

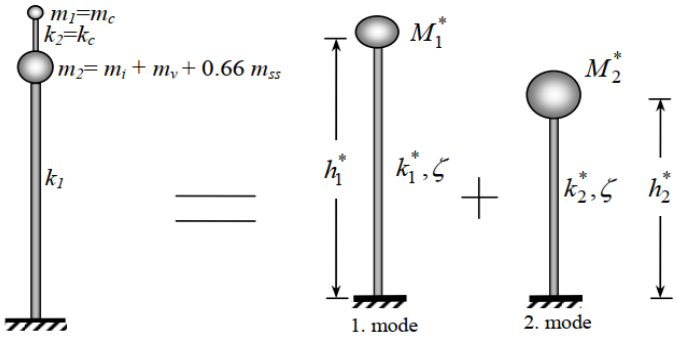

Figure 2: The effective modes of the EWTs model [39].

$$M_n^* = \Gamma_n L_n^h = \frac{(L_n^h)^2}{M_n};\ h_n^* = \frac{L_n^\theta}{L_n^h};\ k_n^* = \omega_n^2 M_n^* \quad (1)$$

where

$$M_n = \emptyset_n^t M \emptyset_n = \sum_{i=1}^{n} m_i \emptyset_{jn}^2 \ :\ \Gamma_n = \frac{L_n^h}{M_n} \ :\ L_n^h = \sum_{i=1}^{n} m_i \emptyset_{jn} :\ L_n^\theta = \sum_{i=1}^{n} h_i m_i \emptyset_{jn} \quad (2)$$

In addition, N is the total number of mode shapes, $\emptyset_n$ is the mode vector of the **nth** mode and **ω_n^2** is the eigenvalue of the **nth** mode. Thus, two single degrees of freedom systems can be used to model the elevated tank. Due to the absolute difference between the lateral stiffness of convective mode k_2 and the staging lateral stiffness k_1, the first and second modes represent the convection and impulsive modes, respectively [40]. Then, the internal forces can be evaluated by combining the impulsive and convective components utilized the absolute summation combination technique as advised by Eurocode-8 [8]. The seismic behavior of the EWTs can be assessed using both standard modal analysis, as previously outlined, and response spectra techniques. The present analysis considers the soil classifications A (rocky soil) and C (medium soil) as defined in Eurocode-8 [41]. The response spectrum values were calculated based on the design damping ratio of 5% using the first curve of the response spectrum that is used for the most seismically active regions in southern Europe. The design ground acceleration (a_g) is considered equal to 0.3 g. For all liquid types, a convective mode damping ratio of 0.5% is recommended.

2.2. Seismic analysis of EWTS according to ACI 350.3-6

The seismic analysis and design processes for concrete structures holding liquids are outlined in ACI 350.3-06 [42]. The model recommended for representing tanks in ACI 350.3-06 is based on the expressions initially developed by Housner [11] with some minor modifications based on various technical standards. The tank's geometry, particularly the D/h ratio, influences the model's parameter values. In ACI 350.3-06 [42], the mathematical expressions proposed for circular liquid storage tanks are provided in Table 2. These equations are valid for such tanks with rigid walls.

Table 2: Circular water tanks design equations [42].

The design equations for circular water tanks.
$\frac{m_i}{m} = \frac{\tanh\left[0.866\left(\frac{D}{H}\right)\right]}{0.866\left(\frac{D}{H}\right)}$
$\frac{m_c}{m} = 0.23\left(\frac{D}{H}\right)\tanh\left[3.68\left(\frac{H}{D}\right)\right]$
$\frac{h_i}{H} = 0.375 \ \text{ for } \frac{D}{H} \geq 1.333$
$\frac{h_i'}{H} = 0.45 \ \text{ for } \frac{D}{H} < 0.75$

$$\frac{h_i'}{H} = \frac{0.866\left(\frac{D}{H}\right)}{2\tanh\left[0.866\left(\frac{D}{H}\right)\right]} - 0.125 \text{ for } \frac{D}{H} \geq 0.75$$

$$\frac{h_c}{H} = 1 - \frac{\cosh\left[3.68\left(\frac{H}{D}\right)\right] - 1}{3.68\left(\frac{H}{D}\right) \times \sinh\left[3.68\left(\frac{H}{D}\right)\right]}$$

$$\frac{h_c'}{H} = 1 - \frac{\cosh\left[3.68\left(\frac{H}{D}\right)\right] - 2.01}{3.68\left(\frac{H}{D}\right) \times \sinh\left[3.68\left(\frac{H}{D}\right)\right]}$$

$$k_c = 3.68\frac{m_c \times g}{D}\tanh\left[3.68\left(\frac{H}{D}\right)\right]$$

This method is appropriate for tanks constructed from reinforced concrete. All Standards for ground-supported tanks and elevated tanks use the two-mass model, with the latter requiring a precise representation of the supporting structure. This structure is typically idealized as a vertical cantilever, as shown in Figure 3, with the staging lateral stiffness k_s and lumped structural mass m_s. This mass comprises the tank container mass along with one-third of the staging mass [6, 9, 10, 42].

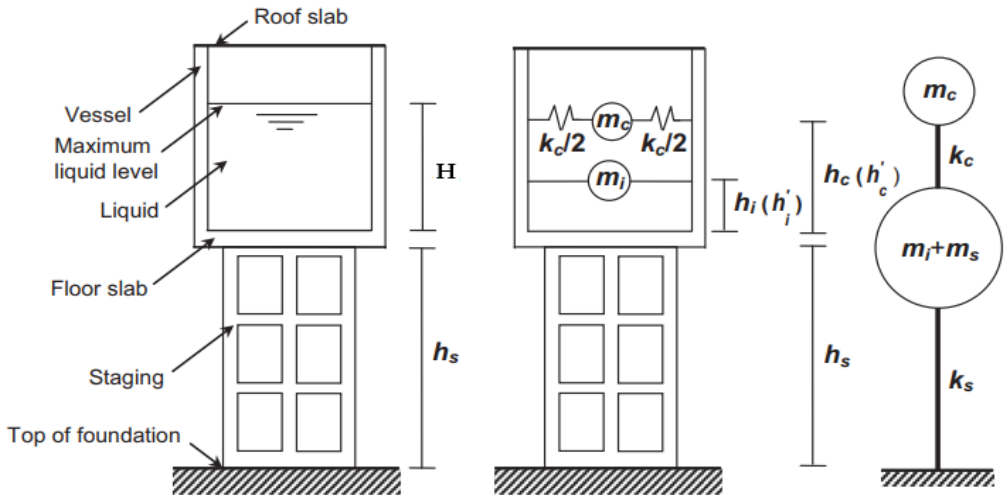

Figure 3:Two-mass idealization for EWTs [43].

The vibration periods of impulsive mode (T_i) and convective mode (T_c) of the equivalent system in seconds are given by:

$$T_i = 2\pi\sqrt{\frac{m_i+m_s}{k_s}} \quad (3)$$

$$T_c = \frac{2\pi}{\sqrt{3.68\tanh\left(3.68\frac{H}{D}\right)}}\sqrt{\frac{D}{g}} \quad (4)$$

According to ASCE 7-16, the ACI 350.3-06 standard [42, 44] are utilized for the design of EWT. Accordingly, equation (5) is used to calculate the base shear (V).

$$V = C_s\,W \quad (5)$$

where C_s is the seismic response coefficient for the impulsive $(C_s)_i$ or convective $(C_s)_c$ mode, and W is the impulsive or convective components' effective seismic weight as determined by Housner's approach [11]. The

following equation is used to get the seismic response coefficient of the impulsive component $(C_s)_i$:

$$\text{For } T_i \le T_s, \qquad (C_s)_i = S_{Ds}\frac{I}{R} \tag{6}$$

$$\text{For } T_i > T_s, \qquad (C_s)_i = \frac{S_{D1}}{T_i}\frac{I}{R} \le S_{Ds}\frac{I}{R} \tag{7}$$

According to ACI 350.3-06, the convective seismic response coefficient $(C_s)_c$ is calculated as follows:

$$\text{For } T_c \le 1.6/T_s, \qquad (C_s)_c = \frac{1.5S_{D1}}{T_c}\frac{I}{R} \le 1.5S_{DS}\frac{I}{R} \tag{8}$$

$$\text{For } T_c > 1.6/T_s, \qquad (C_s)_c = 6\frac{0.4S_{DS}}{T_c^2}\frac{I}{R} \le \frac{2.4S_{DS}}{T_c^2}\frac{I}{R} \tag{9}$$

where the response modification factor is denoted by R, and the importance factor is denoted by I. S_{DS}, which is equal to $\frac{2}{3}F_aS_s$ is the design spectral response acceleration at short periods. S_{D1}, which is equal to $\frac{2}{3}F_vS_1$ is the design spectral response acceleration at 1-s periods. T_s is given by $\frac{S_{D1}}{S_{DS}}$. Ss is the mapped MCER spectral response acceleration at short periods. S_1 is the mapped MCER spectral response acceleration at 1 s period. F_a is the short-period site coefficient (at 0.2 s period). F_v is the long-period site coefficient (at 1.0 s period).

The coefficients S_{DS} and S_{D1} are determined according to ASCE 7-16 provisions. The response values in this investigation are computed so that an importance factor I = 1 and a response modification factor R = 1. This standard recommends combining the convective and impulsive seismic impacts. To determine the total response of the tank, take the square root of the sum of the squares (SRSS) of the convective and impulsive components. To calculate the seismic response for the EWT per ASCE 7-16 specifications, the design spectrum is utilized with a peak ground acceleration of 0.3 g. In addition, the tank location is considered in the Imperial Valley, where the mapped spectral accelerations (S_S and S_1) are considered equal to 1.5 g and 0.6 g, respectively. According to the current investigation, the site is considered to belong to Site Class "A," which is defined by hard rock soil. Additionally, Site Class "D" is considered for Stiff soil conditions.

3. Finite element Modeling

In this study, both the elevated tank construction and the contained liquid are simulated using the Finite Element (FE) approach. ANSYS v13.0 software [45] that combines fluid and structural capabilities, were used to perform modal analysis and evaluate the seismic response of the tank. This study utilizes SHELL 63 elements to model the tank container, featuring four nodes with 6 DOFs each, covering translational and rotational movements, as shown in Figure 4.a. The staging system is represented using the BEAM 188 element, which offers either six or seven DOFs per node, as depicted in Figure 4. b. The fluid domain within the tank is simulated using FLUID 80 elements [46–48], which is an eight-node element having 3 DOFs per node, including translational movements in the three directions, as shown in Figure 4.c. This element is used to model the incompressible fluids that exhibit minimal nodal displacements and no net flow rate. For evaluating fluid-solid interactions, acceleration effects, and hydrostatic pressures, the FLUID 80 element is especially appropriate. The tank container shell and the staging system are modeled using 960 shell elements and 348 beam elements, respectively. For the various tank fill levels considered in this study, including quarter, half, three quarters, and full, the fluid model utilizes 1296, 2160, 3888, and 4320 fluid elements, respectively.

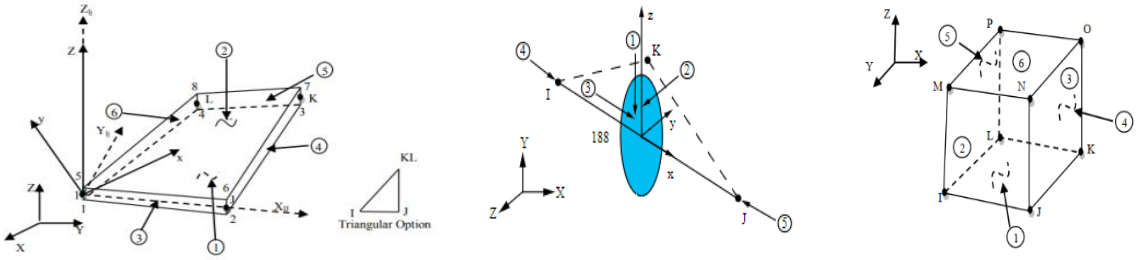

(a) Shell 63 (b) Beam 188 (c) Fluid 80

Figure 4: FE geometries of (a) Shell 63, (b) Beam188, (c) Fluid 80 [45].

The modern research has shifted towards more advanced methods including finite element FE modeling is now widely used in structural modelling. These numerical techniques enable detailed simulation of complex phenomena like fluid-structure interaction (FSI). The FSI approaches, including Coupled Eulerian-Lagrangian (CEL), Arbitrary Lagrangian–Eulerian (ALE), Coupled acoustic-structure (CAS), Smoothed Particle Hydrodynamic (SPH) methods, etc., can be used to formulate fluid-structure interaction problems. In this study, the displacement-based Lagrangian method is chosen to simulate the interaction between the elevated tank and the contained fluid. The interaction between the fluid and the tank container is considered by implementing proper coupling at the nodes situated on the fluid-structure interface [47]. The coordinate system is defined such that the radial, circumferential, and vertical directions correspond to the global X, Y, and Z-axes, respectively. Nodes along the tank circumference are constrained in the radial direction, and those at the base are fixed vertically, ensuring that the fluid remains bounded by the tank walls and bottom while allowing transverse motion. Finally, the FE model of the elevated tank is subjected to a full transient linear dynamic analysis. The governing equation of motion for transient analysis is expressed as follows:

$$(\mathbf{M})\{\ddot{\mathbf{u}}\} + (\mathbf{C})\{\dot{\mathbf{u}}\} + (\mathbf{K})\{\mathbf{u}\} = \{\mathbf{F(t)}\} \quad (10)$$

where M, C, and K are the mass, damping, and stiffness matrices of the structure, and {ü}, {u̇}, and $\{u\}$ denote the nodal acceleration, velocity, and displacement vector, respectively, and {F(t)} is the load vector. The transient response is computed in ANSYS software using Newmark's direct time-integration method.

4. Verification of the FE model

To validate the model tank, a modal analysis of a conical EWT is performed using the present FE approach, and the results are compared with those reached by Moslemi et al [16]. Moslemi analyzed a conical EWT supported on a concrete shaft with a hinged base, considering both tank-wall flexibility and water sloshing effects. The tank model, located in the United States, has a storage capacity of 7,571 m³. Figure 5 illustrates the tank geometry and FE model, while **Error! Reference source not found.** summarizes its geometric properties.

Table 3: Tank geometric characteristics

Property	Value	Property	Value
Side shell thickness (mm)	8.8	Tank floor thickness (mm)	330
Cone thickness (mm)	24.5	Shaft thickness (mm)	380

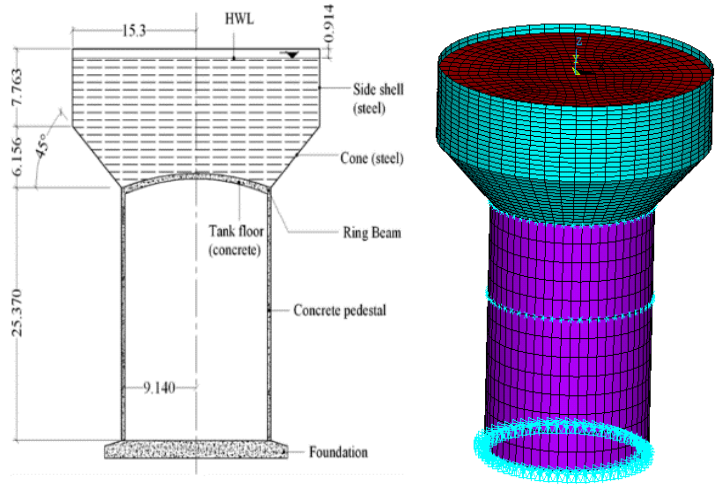

(a) (b)

Figure 5: Conical EWT model geometry (a) EWT geometry[49], (b) FE idealization for the EWT model

To take into account the similar weight of the shaft's platforms with their entire live load, a mass is applied and distributed at a height of 15.6 m above the base, estimated at 715 $\times 10^3$ kg. Furthermore, a mass

distributed around the ring beams was added to reward the weight of the ingredients not represented in the FEM and this mass is estimated to be 438 $\times 10^3$ kg. The contained water within the tank was used with density and a bulk modulus (K) equal to 1000 kg/m^3 and 2.1 GPa, respectively. The elements of steel and concrete were represented as linear elastic materials with the characteristics given in Table 4.

Table 4: characteristics of steel and concrete materials

Property	Steel material	Concrete material
Young's modulus (GPa)	200	24.86
Poisson's ratio	0.30	0.16
Density (kg/m3)	7898	2400

Based on the highest participation factors of both impulsive and convective modes, Table 5 displays the natural frequencies that correspond to their predominant mode shapes. Ri (%) is the effective modal mass in the X direction divided by the system's total mass. The results of the FE model exhibit remarkable concurrence with the results of Moslemi et al. [16]. The mode shapes correspond to the modes listed in Table 5 are illustrated in Figure 6 and Figure 7.

Table 5: Results of modal analysis for the EWT model

mode		Moslemi et al [16]			Current study		
Number	Type	Frequency (Hz)	Effective mass*10^3 (KG)	Ri (%)	Frequency (Hz)	Effective mass*10^3 (KG)	Ri (%)
*1	Convective	0.161	4302.51	58.7	0.158	4557.82	58.7
2		0.161	235.38				
3		0.294	141.63		0.288	119.277	
1	Impulsive	1.955	918.36	41.3	1.9123	4300.81	41.3
*2		1.955	3367.52				
3		7.470	228.14				
4		7.470	561.35		7.142	645.600	
5		8.560	308.23				

* Fundamental mode

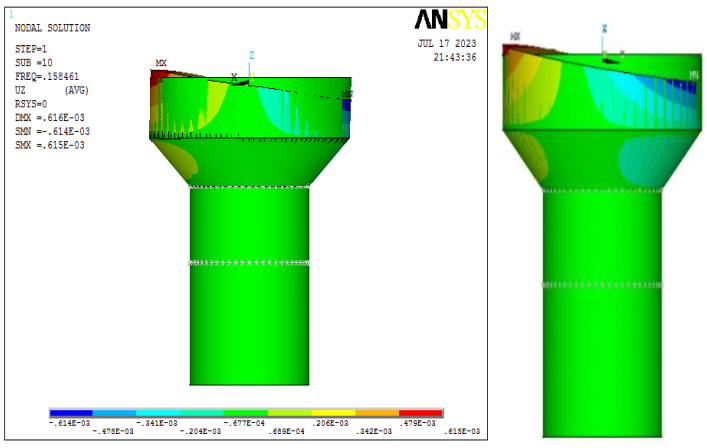

(a)

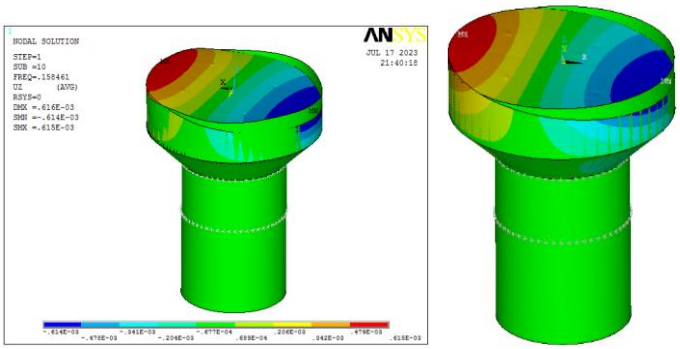

(b)

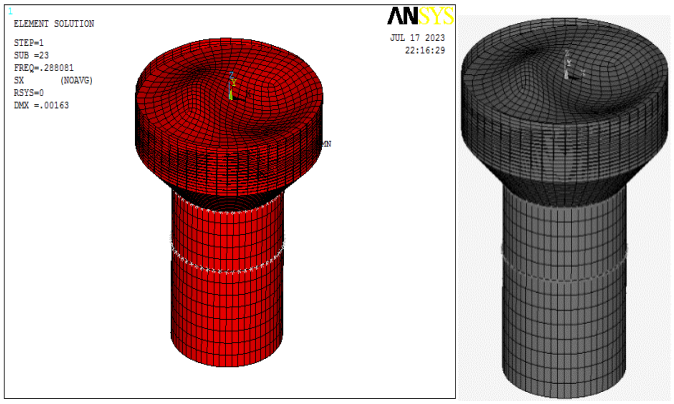

(c)

Figure 6: Convective modes for EWT, (a) Side view (Mode 1); (b) 3D view (Mode 1); (c) 3D view (Mode 3) [49].

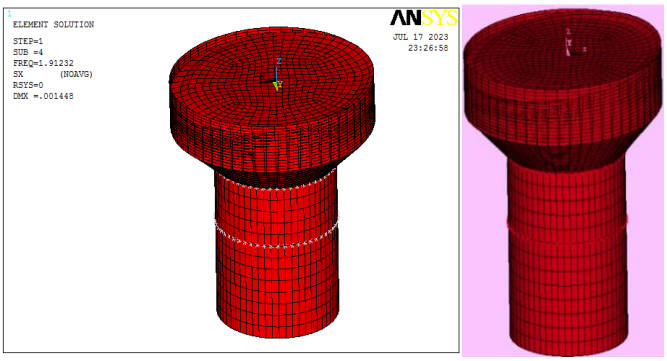

(a)

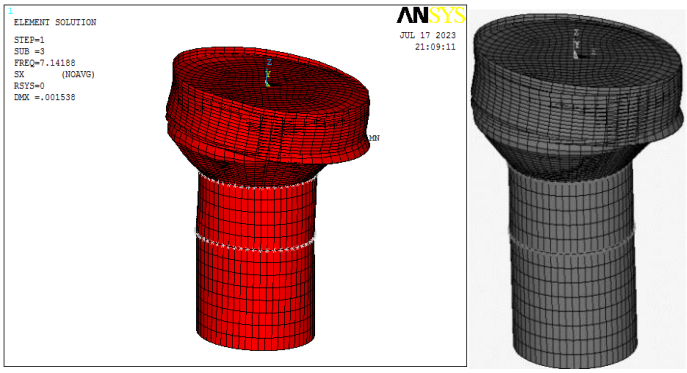

(b)

Figure 7: Impulsive modes for EWT, (a) 3D view (Mode 2), (b) 3D view (Mode 4) [49].

To verify the time history analysis of the EWT, the tank model was subjected to El-Centro earthquake with a peak ground acceleration of 0.31 g. The maximum base shear and overturning moment were calculated and compared with the results obtained by Moslemi [16]. As shown in

Table *6*, the results exhibit strong agreement, confirming that the present FE model accurately represents the seismic behavior.

Table 6: Absolute maximum values of time history response for the EWT model

	Moslemi et al [16]	Current study	Difference (%)
Max Base shear (kN)	34 842	34 101	1.02
Max Base moment (kN m)	1 293 880	1 198 540	1.08

5. Experimental validation

For a more accurate assessment of current study, an experimental study is conducted to verify the validity of numerical models. A simple experiment is prepared to determine the Fundamental convective and impulsive frequency for the Lab EWT models for Quarter full and half full cases. To determine the fundamental frequency of the EWT, the Digital Image Correlation (DIC) is used. To capture the model's motion, a high-speed camera set to 240 FPS frames per second was employed. This non contact measurement simplifies the experiment to produce results comparable to those usually obtained with high-precision sensors. To obtain the frequency of the model, the initial displacement of the model is given and left to vibrate freely, with several videos recorded for that motion to get the frequency of the model. Using Matlab software, these videos were analyzed to get displacement, and then the continuous wavelet transformation (CWT) is applied to get the desired frequencies.

5.1 Experimental Model Description

The cylindrical tank experimental model has a diameter of 250 mm, a height of 230 mm, and a wall thickness of 1.5 mm; it contains water with a density $\rho = 1000$ Kg/m^3 and a bulk modulus $\beta = 2.1$GPa. The container tank is made of polypropylene (PP) and is mounted on an 8 mm thick wooden base, which is supported by a Teflon (PTFE) staging. This staging consists of four columns each with a diameter of 17 mm. The Distance between the centers of each column for the other 120 mm, with the base plate being made of 5 mm thick aluminum plate. There are no horizontal bracings and the tank is supported on a 450 mm-high staging as shown in Figure 8. The material properties used in this model are summarized in Table 7. This practical model represents a prototype of a tank made of reinforced concrete of 4.6 m height and 5 m diameter. The tank's wall has a thickness of 120 mm, while the floor is 200 mm thick. It is supported by a staging frame that stands at a height of 9 m. This staging comprises four columns, each with a diameter of 450mm, and horizontal beams measuring 300 x 450 mm located at two different levels, modeled as a linear elastic material with a Modulus of elasticity (E) of 22.36 GPa, Poisson's ratio (μ) of 0.2, and density of 25 kN/m^3. The experimental model tank response is assumed to have stayed within the elastic range. To satisfy the similitude requirements, the Buckingham π theorem [50] and the Cauchy number [51] are used. There are three important dimensions to making a scale for the experiment model: length, mass, and time. The length scale factor (SF_{Length}) is equal to the ratio between the radius of the tank (prototype/model), and also the mass factor (SF_{Mass}) is equal to the ratio between the mass of store the liquid (prototype/model) and The time scale factor (SF_{Time}) is defined by the ratio of the Time period of the impulsive mode (prototype/model). The acceleration scale factor (SF_{Accel}) is determined from (SF_{Length}) and $(SF_{Time})^2$. The stiffness scale factor (SF_{Stiff}) is depends on the similitude between (SF_{Mass}), (SF_{Accel}), and (SF_{Length}). The scale factors for the experiment are shown in Table 8.

Table 7: Material Properties Used in the Experimental Model

Material	Density (kg/m3)	Young's modulus (GPa)	Poisson's ratio

Polypropylene (PP)	900	1	0.4
Wood	800	3	0.3
PTFE (Polytetrafluoroethylene)	2100	1.225	0.46

Table 8: Scale factors for the experiment.

Physical quantity	Similitude	prototype
Length (SF_{Length})	$SF_{Length}= R_{pro} /R_{mod}$	20
Mass (SF_{Mass})	$SF_{Mass}= M_{pro} /M_{mod}$	8000
Time (SF_{Time})	$SF_{Time}= Ti_{pro}/ Ti_{mod}$	3.1
Acceleration (SF_{Accel})	$SF_{Accel} = SF_{Length}/ SF_{Time}^2$	2.08
Stiffness (SF_{stiff})	$SF_{stiff} = SF_{Mass}* SF_{Accel}/ SF_{Length}$	832
Stress (SF_{stress})	$SF_{stress} = SF_{Mass}* SF_{Accel}/ SF_{Length}^2$	41.6

This experimental study aims to determine the fundamental natural frequency of the tank system for two water levels: quarter full (55 mm) and half full (115 mm), with the base considered fixed. Figure 9 shows the results of the Continuous wavelet transform (CWT) for both filling cases. Since it was difficult to identify the dominant frequency from the 3D CWT figure, as illustrated in Figure 9, then a section is extracted from each CWT for accurate frequency determination as shown in Figure 10. Two dominant frequencies are observed: the impulsive frequency, associated with the bottom mass and characterized by erratic behavior, and the convective frequency, associated with surface sloshing due to upper mass movement. Table 9 represents the fundamental natural periods of the tank system obtained from numerical finite element analysis using ANSYS, the experimental results and code-based calculations. The results indicated that increasing the liquid mass leads to a decrease in the fundamental impulsive natural frequency and increase in the fundamental convective natural frequency.

Figure 8 : Experimental Model.

Table 9 shows good agreement between experimental, numerical results and codes formulas, with a difference of less than 10% except the impulsive frequency for the codes formulas which exceeds 10%. Figure 11 shows the

fundamental convective frequency obtained from experimental results with corresponding FE results for both filling cases.

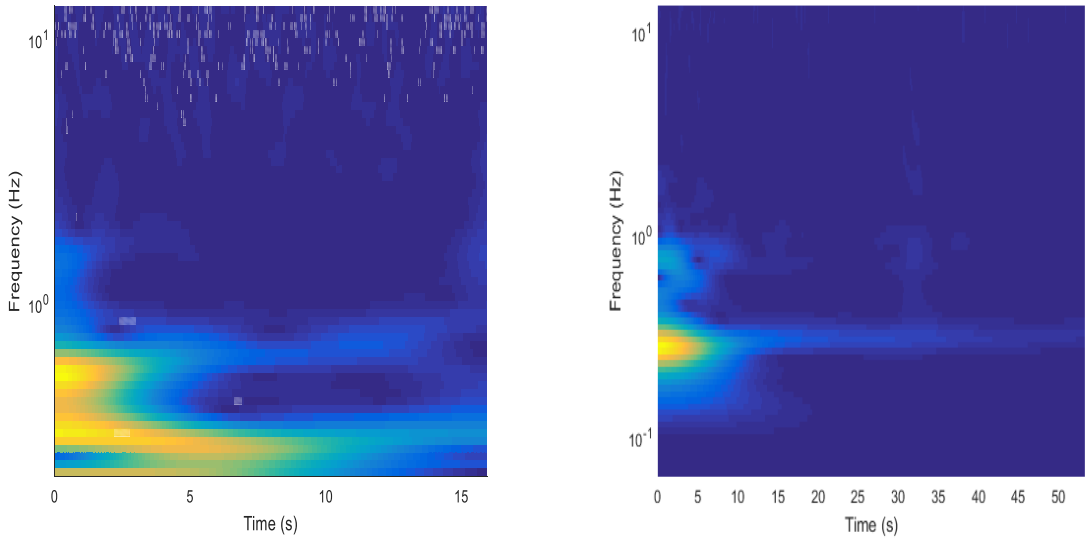

(a) (b)

Figure 9: CWT of EWT for different fullness level (a) quarter full (b) half full

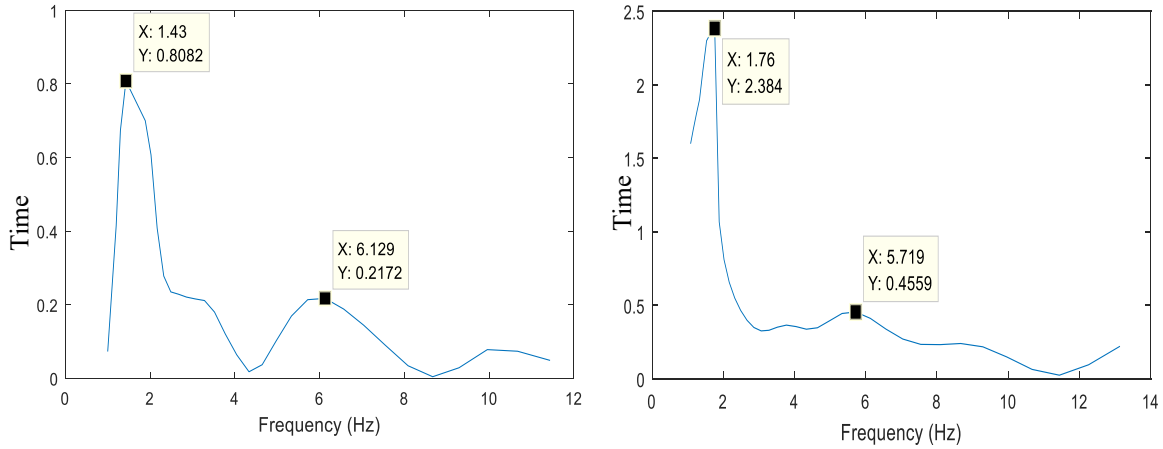

(a) (b)

Figure 10: CWT section of EWT for different fullness level (a) quarter full (b) half full.

(a)

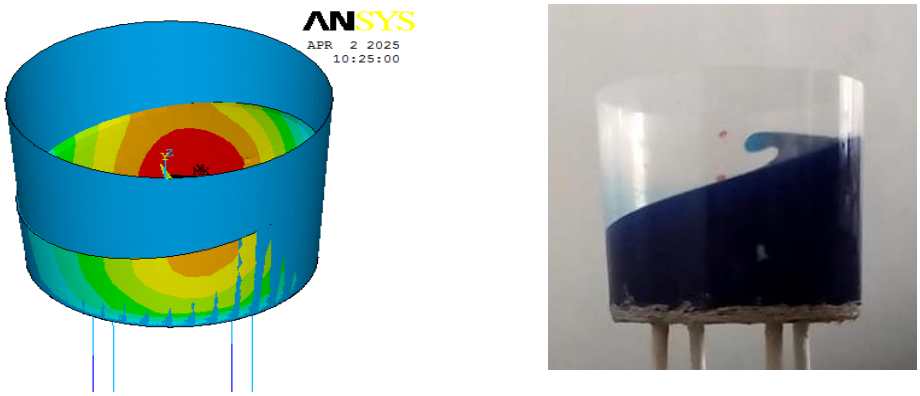

(b)

Figure 11: Resonance at convective frequency (a) Quarter full Case; (b) Half-Full Case.

Table 9: Comparison of First Natural periods: FEM, Practical Tank Model and Codes.

	FE		EXP		Eurocode 8		ACI 350.3-06	
	1st Convective	1st Impulsive	1st Convective (% Error)	1st Impulsive (% Error)	1st Convective (% Error)	1st Impulsive (% Error)	1st Convective (% Error)	1st Impulsive (% Error)
Quarter Tank	0.669	0.162	0.699 (4.4 %)	0.163 (0.6 %)	0.676 (1.0 %)	0.17 (4.9 %)	0.66 (1.3 %)	0.162 (0.0 %)
Half Tank	0.595	0.186	0.568 (4.5 %)	0.175 (5.9 %)	0.562 (5.5 %)	0.212 (13.9 %)	0.556 (6.5 %)	0.226 (21.5 %)

6. Comparative case study

To perform the present study, the EWT shown in Figure 12 is analyzed. This tank is circular with a capacity of 55 m³. It has a diameter of 4.85 m and a height of 3.3 m, which includes a freeboard of 0.3 m. The tank's wall has a thickness of 120 mm, while the floor is 200 mm thick. It is supported by a staging frame that stands at a height of 14m. This staging comprises four columns, each with a diameter of 450mm, and horizontal beams measuring 300 x 450 mm located at four different levels. The tank is constructed using reinforced concrete, modeled as a linear elastic material with a Modulus of elasticity (E) of 22360 MPa, Poisson's ratio (μ) of 0.2, and density of 25 kN/m^3.

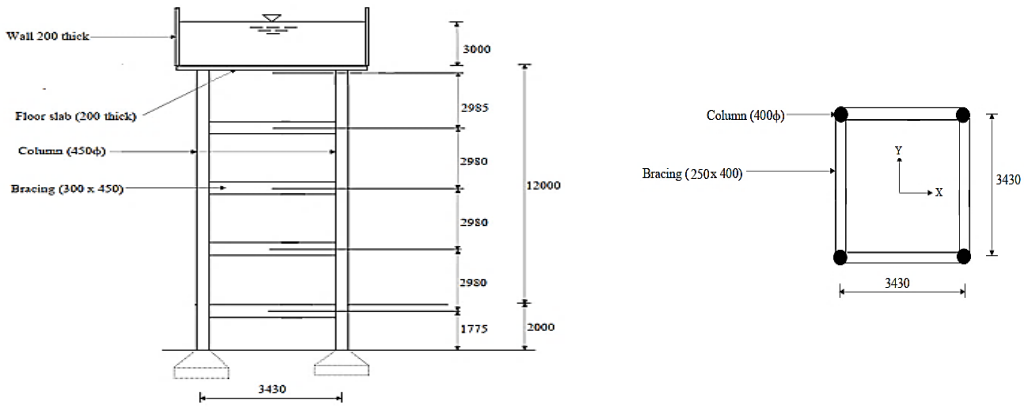

(a) **(b)**

Figure 12: EWT geometry (a) Elevation; (b) Plan of staging [9].

The contained water within the tank is considered to have a bulk modulus (K) of 2.1 GPa and a density of 1000 kg/m^3. The response of the EWT during earthquakes is influenced by the nature of the supporting soil. Therefore, the supports at the staging base are considered fixed if the supporting soil is rocky. Conversely, the base is considered hinged if the supporting soil is of medium consistency. Table 10 shows ground types and associated shear wave velocities as outlined in codes such as Eurocode-8 and ASCE 7-16.

Table 10: Ground types defined in the Eurocode-8 and ASCE 7-16

	Eurocode-8	ASCE 7-16	
Ground types	Description of soil	Ground types	Description of soil
A	Rock $V_{s,30}$>800 m/s	A	Hard rock V_s > 5,000 ft /s
C	Deep deposits ranging in thickness from a few tens to several hundreds of meters that include stiff clay, dense or medium-dense sand, or gravel $V_{s,30}$ ≈180~360	D	Stiff soil V_s > 600 to 1,200 ft /s

Two types of analyses are performed to study the seismic response of EWT considering fluid structure interaction: (1) modal analysis and (2) time history analysis. As seen in Figure 13, the model is analyzed for four different tank capacity levels.

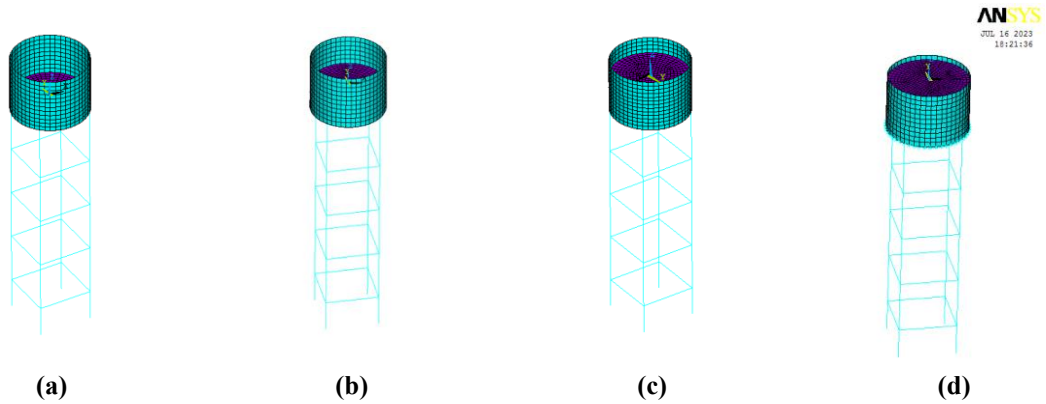

Figure 13: Elevated tank FE model cases (a) Quarter full (b) Half Full (c) Three quarters full (d) Full

7. Modal analysis

Modal analysis is conducted on the elevated tank models, considering both fixed and hinged bases, using the reduced method in ANSYS (MODOPT, REDUCED) [45]. Four tank capacities were analyzed. Table 11 presents the fundamental natural frequency of the impulsive and convective modes dependent on the mass participation factors, In addition, the corresponding values determined using Eurocode 8 and ACI 350.3-06 formulas.

Table 11: Comparison of the fundamental natural frequencies (Hz): ANSYS, and different codes for different filling percentages (1st convective frequency (f_c) and 1st impulsive frequency (f_i))

Filling Case	Support case	FE		Eurocode 8		ACI 350.3-06	
		(f_c)	(f_i)	(f_c)	(f_i)	(f_c)	(f_i)
Quarter	Fixed base	0.309	1.597	0.311	1.403	0.312	1.58
	Hinged base	0.309	1.587	0.311	1.298	0.312	1.466
Half	Fixed base	0.383	1.493	0.388	1.357	0.392	1.486
	Hinged base	0.383	1.376	0.388	1.25	0.392	1.369
Three quarters	Fixed base	0.405	1.372	0.413	1.272	0.42	1.368
	Hinged base	0.405	1.267	0.413	1.177	0.42	1.266
Full	Fixed base	0.413	1.263	0.422	1.195	0.429	1.256
	Hinged base	0.413	1.17	0.422	1.11	0.429	1.163

As can be noticed, as the tank filling percentage rises, the natural frequency of the tank (f_i) decreases. This phenomenon is mainly caused by the increased water impulsive mass vibrating with the tank. The fundamental frequency of both the impulsive (f_i) and convective (f_c) modes obtained using FE analysis for different tank filling percentages are compared with various international codes of practice, as shown in Table 11. The frequency of impulsive mode (f_i) from the FE analysis aligns more closely with ACI 350.3-06 than with Eurocode 8. The frequency of convective mode (f_c) using FE analysis is found to be consistent with Eurocode 8 in comparison to ACI 350.3-06, showing only a minor discrepancy not exceeding 2%.

8. Time history analysis

The seismic behavior of the EWT models is investigated using time history analysis. The studied EWT is subjected to three Imperial Valley ground motions El-Centro (1940), Aeropuerto Mexicali (1979), and Agrarias (1979) for each tank container filling condition. The three records are displayed in Figure 14, and their main characteristics are listed in Table 12. A time step of 0.002s is employed to accurately characterize the seismic response. Damping ratios for the convective and impulsive modes are set at be 0.5% and 5%, respectively. Using the direct time integration technique, time history responses of the EWT models are determined under the impact of these earthquakes. Subsequently, base shear and base moment maximum absolute values are compared to those derived from response spectrum analyses, based on various international codes such as Eurocode 8, ACI 350.3-06 for EWTs. The obtained results are based on the impulsive and convective fundamental modes listed in Table 11. The results are presented in Figures (15, 16,18 and 19).

Table 12: Ground motion characteristic

Different ground motions	Event	Year	Station	Magnitude Mw	Time steps (s)	Total time period (s)	PGA (g)
El-Centro	Imperial Valley	1940	El Centro Array #9	6.9	0.02	31.14	0.31
Aeropuerto Mexicali		1979	Aeropuerto Mexicali	6.53	0.02	14.74	0.31
Agrarias		1979	Agrarias	6.53	0.02	28.41	0.3

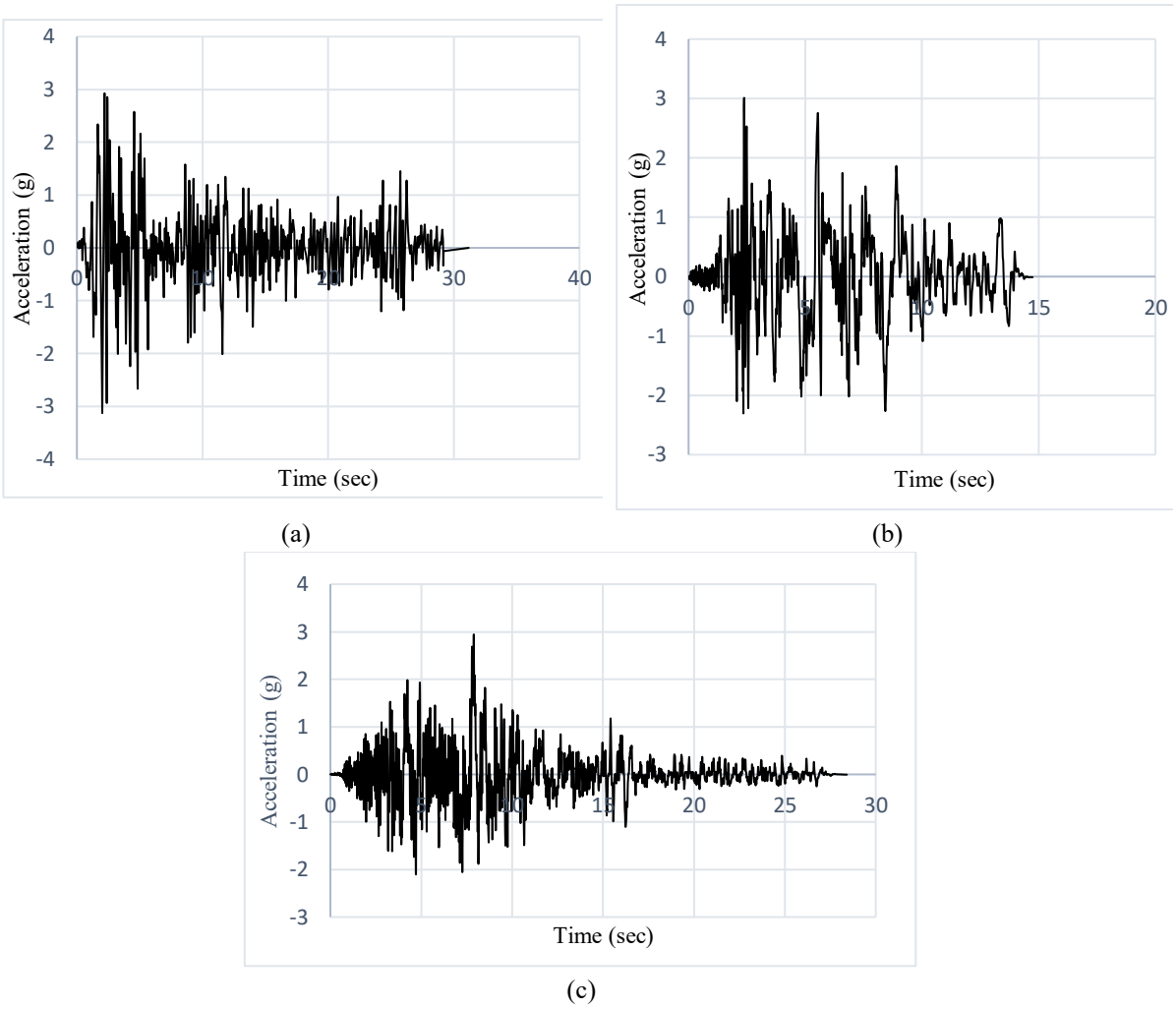

Figure 14: Time history of ground motions (a) El-Centro earthquake; (b) Aeropuerto Mexicali earthquake; (c) Agrarias earthquake.

Figures 15 and 16 illustrate the maximum base shear and overturning moment responses of the EWTs for the different filling cases. The FE analysis results are compared with those obtained from international design codes, i.e., Eurocode 8, ACI 350.3-06 with ASCE 7-16. The responses increase as the storage tank fill percentage approaches half-full; however, they decrease again as the tank reaches full capacity. This increase is not strictly linear but is influenced by the inherent characteristics of the system. The FE results show that the base shear and overturning moments are greater when the tank is half-full or three-quarters full. This is attributed to the increased hydrodynamic pressures resulting from the acceleration of the liquid within the tank container. As shown in Figures 15 and 16, the El-Centro earthquake on the EWT models with fixed base gives the maximum response occurs when the container of the tank is half–full, While in the case of the other two earthquakes, the Aeropuerto Mexicali earthquake and the Agrarias earthquake give the maximum response when it fills a Three-quarters full. Many previous studies and researches show that the critical condition is not always in the case of full filling [23–25, 52–57]. Across various international codes, the peak response occurs in the scenario of a full tank primarily due to the increased water mass within the tank container as the fill level rises, without considering the impact of water sloshing. Figures 15 and 16 also illustrate the results of the different international codes, using the elastic response spectrum method, to investigate the behavior of EWTs under different cases of tank filling. The different international codes consistently underestimate the results across various filling scenarios, except for the full tank case. Consequently, the elastic response spectrum method, advocated by international codes, appears to offer a less precise estimation of the seismic response for EWTs, particularly across varied filling conditions. Then, it is essential to account for the sloshing effect of the water's free surface in both the analysis and design phases of

storage tanks. Although the codes used El-Centro earthquake in constructing the response spectrum, and the FE analysis used the same earthquake, the high difference between these results pronounce the essential effect of water sloshing in the analysis and design of EWT. The results indicate that the natural period of the EWT system at one quarter and three quarters filling levels shows a convergence between the El-Centro and Agrarias earthquake responses, but compared to the Aeropuerto Mexicali earthquake gives a lower response, as confirmed in Figures 15 and 16. Moreover, when the tank is half-full, the response to the El-Centro earthquake is higher than that of the other two earthquakes, which makes it more responsive to the system under this condition. Figure 17 shows a comparison between the spectrum of response for each earthquake record used in this study with the natural frequency for different filling cases of EWT with fixed-base. As for the case of the full filling of the container tank, the response for the Aeropuerto Mexicali earthquake is higher than the other two earthquakes, due to the effect of the second impulsive mode, which contributes to the total seismic response of the system based on the data presented in Table 13.

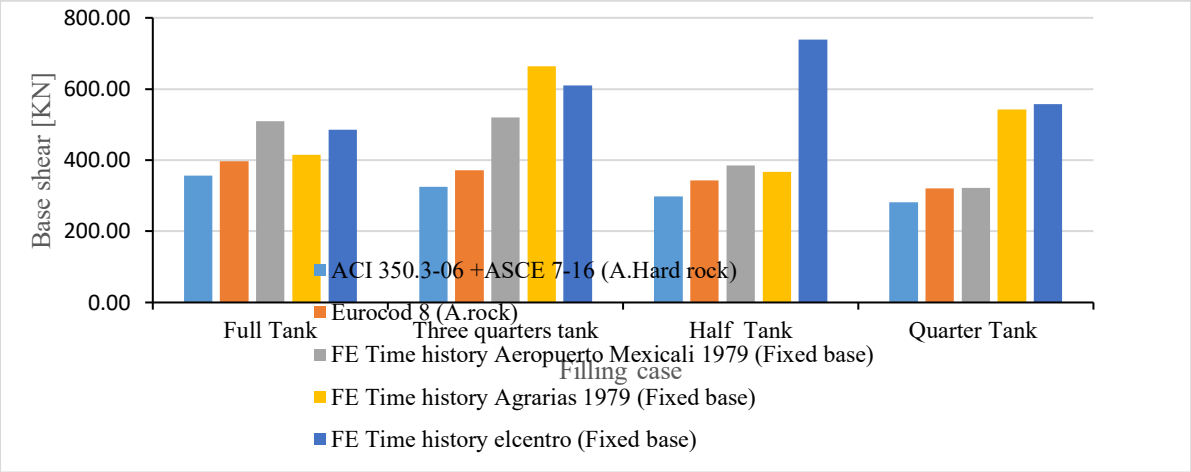

Figure 15: Comparison of maximum base shear forces (ANSYS and different codes) per filling percent when the supporting soil is rocky.

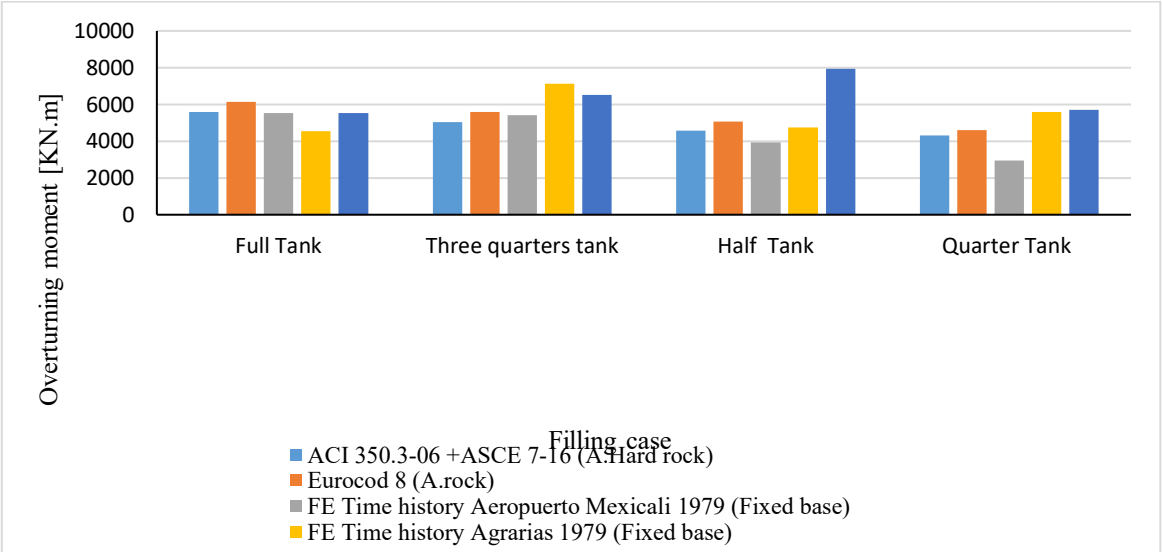

Figure 16: Comparison of the maximum base overturning moment (ANSYS and different codes) per filling percent when the supporting soil is rocky.

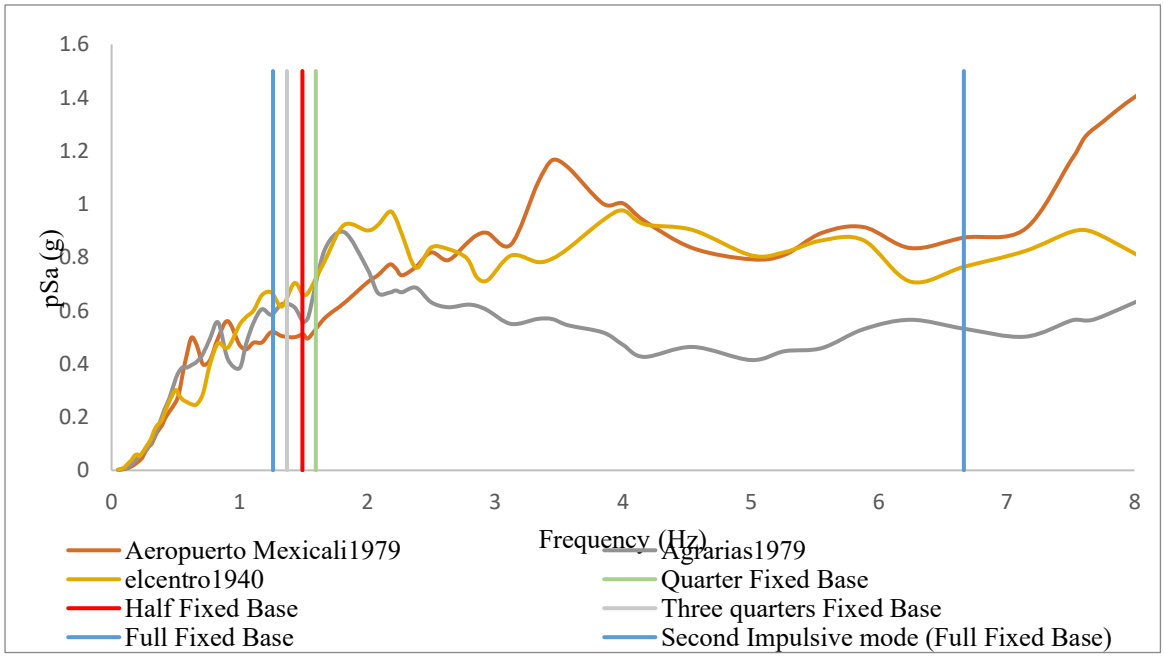

Figure 17: Comparison of the spectral response of earthquake records with the natural frequency for different filling cases of the EWT with a fixed base

Figures 18 and 19 illustrate the comparison between the FE analysis results of EWT models with flexible-base, under the effect of the three different earthquakes and the corresponding values derived from ACI 350.3-06 in conjunction with ASCE 7-16, and Eurocode 8. In this case, the maximum responses occur when the tank is fully filled, which is consistent with the predictions of the international design codes. Figure 20 compares the natural frequency for different EWT filling cases with a flexible base with the spectrum of response for each earthquake record considered in this investigation. When the EWT is in the case of filling the container tank to a quarter as well as, the case of the Three quarters filling, noticed that the system response to the El-Centro earthquake is the highest, then the following Aeropuerto Mexicali earthquake due to the effect of the Higher impulsive mode on the total seismic response of the system. In contrast, in the case of a half-filled tank, the Aeropuerto Mexicali earthquake is less responsive to the system than the other two earthquakes. Figure 21 displays the primary modes for the EWT with a fixed base for all filling cases. According to this analysis, the partnership between the four modes of the structure adds up to over 90%. Convective modes are related to the first and second modes, while impulsive modes are associated with the third and fourth modes.

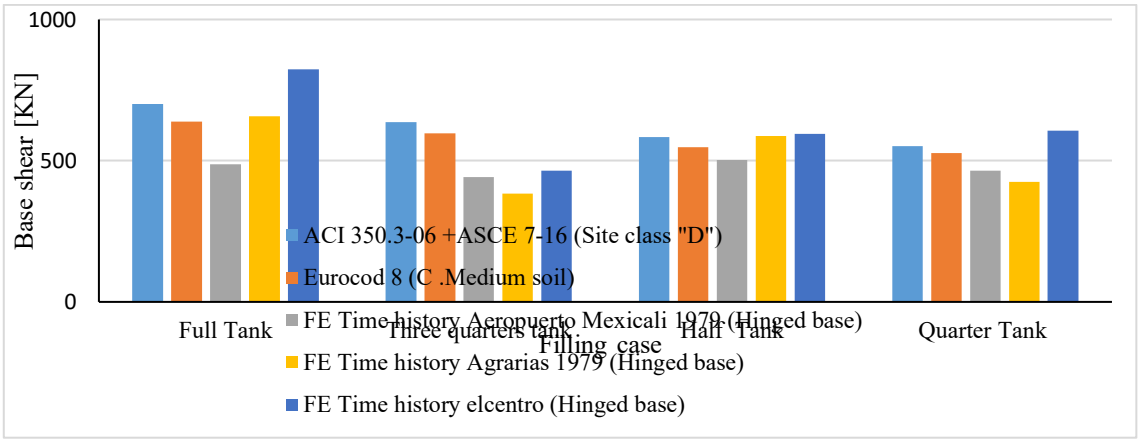

Figure 18: Comparison of the maximum base shear forces (ANSYS and different codes) per filling percent when the supporting soil is of medium consistency.

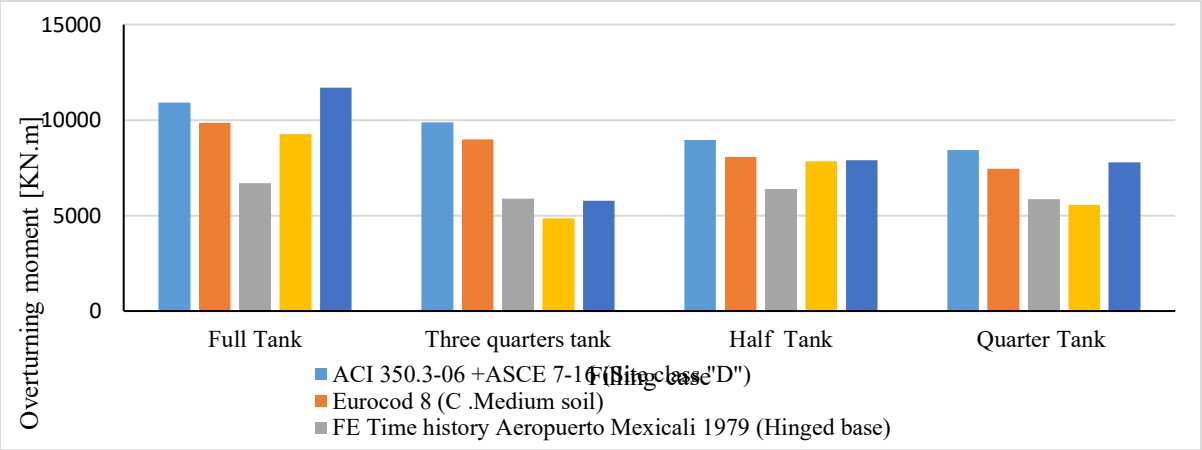

Figure 19: Comparison of the maximum base overturning moment (ANSYS and different codes) per filling percent when the supporting soil is of medium consistency.

Table 13: Free vibration analysis results

mode		Full tank (Fixed base)			Three Quarters tank (Hinged base)			Quarter tank (Hinged base)		
Number	Type	Time period	Effective mass (KG)	Ri (%)	Time period	Effective mass (KG)	Ri (%)	Time period	Effective mass (KG)	Ri (%)
*1	Convective	2.415	24404.3	18.82	2.47	23166.8	19.92	3.242	11378.7	12.94
2		1.431	1098.47		1.417	1119.33		1.4572	825.19	
*1	Impulsive	0.792	91844	74.26	0.602	31326.7	72.77	0.683	68775.2	81.49
**2		0.154	8927.7		0.789	38320.5		0.172	8069.83	
3		-	-		0.788	10333.7		-	-	
4		-	-		0.176	8702.85		-	-	

* Fundamental mode
** Fundamental mode for Three Quarters tank (Hinged base)

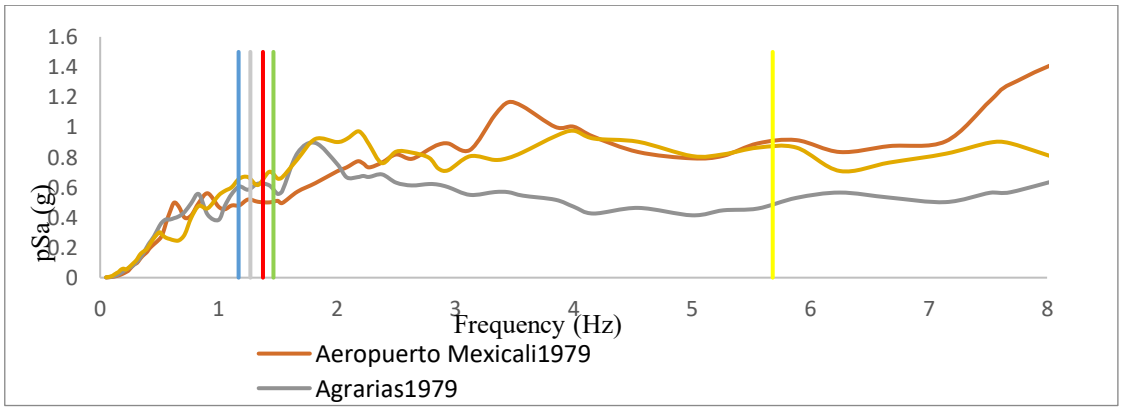

Figure 20: Comparison of spectral response of earthquake records with natural frequency for different filling cases of the EWT with Hinged base.

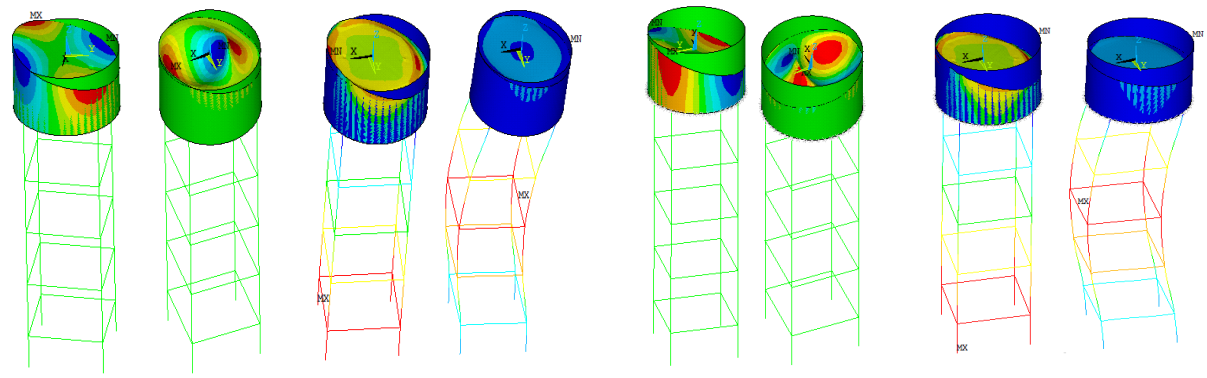

(a.1) Convective modes (a.2) Impulsive modes (b.1) Convective modes (b.2) Impulsive modes

(a) (b)

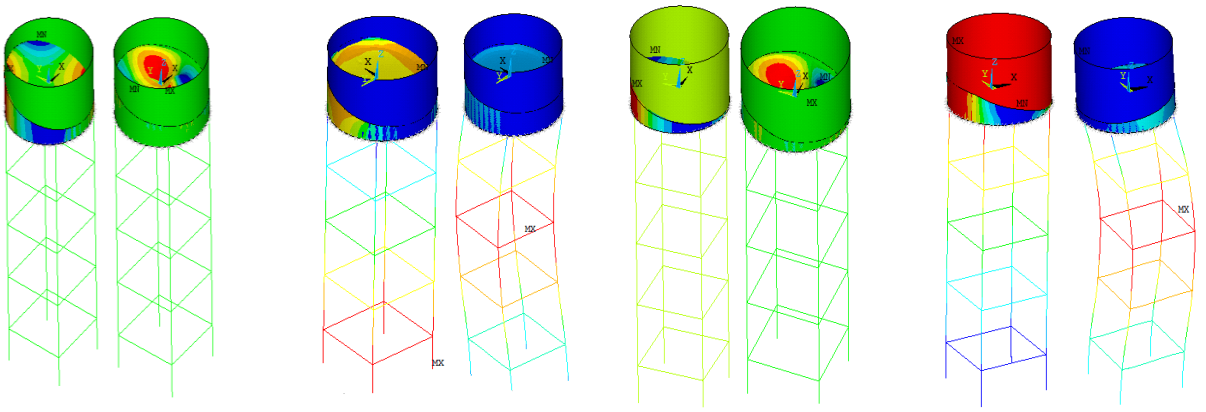

(c.1) Convective modes (c.2) Impulsive modes (d.1) Convective modes (d.2) Impulsive modes

(c) (d)

Figure 21: Mode Shapes for EWT in the model cases (a) Full (b) Three-quarters full (c) Half-Full (d) Quarter full.

9. Conclusions

This study evaluates the seismic analysis procedures of Eurocode 8, ACI 350.3-06, and ASCE 7-16 for circular EWTs at each different filling condition of container tank using a comprehensive FE analysis, with results validated through both experimental and numerical means. Simplified mechanical models based on international codes are compared with FE results. The principal conclusions can be summarized as follows:

- The maximum seismic response of EWTs does not always occur when the tank is completely full. The most critical responses were observed at intermediate filling, especially under fixed-base settings, due to the substantial hydrodynamic pressure generated by sloshing effects in partially filled tanks. This behavior arises when the dominant earthquake frequencies coincide with the natural period of the tank liquid system. The impacts are insufficiently represented by code-based elastic response spectrum approaches, which often underestimate seismic demands for partially filled tanks due to oversimplified assumptions (single impulsive/convective mode, rigid wall assumptions, and disregard for higher modes, e.g.).
- The results indicates that tank wall and base flexibility, and sloshing effects, significantly influence the seismic performance of EWTs and must be taken into account during the design process. system's behavior may not be entirely represented by the fundamental impulsive and convective modes alone,

when higher impulsive modes become active during strong seismic excitations.

In conclusion, while international design codes such as Eurocode 8 and ACI 350.3-06 provide a generally conservative estimation for fully filled tanks, their simplified assumptions limit their accuracy under varying operational conditions. These findings highlight the necessity of accounting for critical parameters including the filling level, earthquake characteristics, and the nature of the supporting soil, as well as performing time-history assessments.

10. Future recommendations

This section presents recommendations aimed at identifying the optimal conditions for applying current code methodologies, while also offering clear, comprehensive, and more accurate insights into the study, below are several recommendations:

- **Extended Parametric Investigation:** Future studies should encompass a broader range of parameters, including various tank geometries, wall thicknesses, staging configurations, liquid depths, aspect ratios, construction materials, shaft geometries, and ground motion characteristics. This can be achieved through the careful selection and modeling of a wide range of liquid storage tanks to investigate the influence of these parameters on the dynamic response of such structures.
- **Enhancement of International Seismic Codes:** Given the identified discrepancies between code predictions and analytical results, it is recommended that international design codes be refined to more accurately address sloshing effects and partial-fill conditions, which are often oversimplified in current formulations.

References

1. Rai DC (2003) Performance of elevated tanks inMw7.7 Bhuj earthquake of january 26th, 2001. J Earth Syst Sci 112:421–429. https://doi.org/10.1007/BF02709269
2. Soroushnia S, Tafreshi ST, Omidinasab F, et al (2011) Seismic performance of RC elevated water tanks with frame staging and exhibition damage pattern. Procedia Eng 14:3076–3087. https://doi.org/10.1016/j.proeng.2011.07.387.
3. Seleemah AA, El-Sharkawy M (2011) Seismic response of base isolated liquid storage ground tanks. Ain Shams Eng J 2:33–42. https://doi.org/10.1016/j.asej.2011.05.001.
4. Sezen H, Livaoglu R, Dogangun A (2008) Dynamic analysis and seismic performance evaluation of above-ground liquid-containing tanks. Eng Struct 30:794–803. https://doi.org/10.1016/j.engstruct.2007.05.002.
5. Chaduvula U, Patel D, Gopalakrishnan N (2013) Fluid-structure-soil interaction effects on seismic behaviour of elevated water tanks. Procedia Eng 51:84–91. https://doi.org/10.1016/j.proeng.2013.01.014.
6. ACI Committee 371 (2008) Guide for the Analysis , Design , and Construction of Elevated Concrete and Composite Steel-Concrete Water Storage Tanks (ACI 371R-08). Farmington Hills, MI, USA
7. Committee ACI (2007) Seismic Design of Liquid-Containing (ACI 350 . 3-06)
8. European Committee for Standardization (CEN) (2006) Eurocode 8: Design of Structures for Earthquake Resistance – Part 4: Silos, Tanks and Pipelines (EN 1998-4:2006). London, UK
9. Sudhir K. Jain AORJ (2007) IITK-GSDMA Guidelines for Seismic Design of Liquid Storage Tanks: Provisions with Commentary and Explanatory Examples. National Information Center of Earthquake Engineering (NICEE), Indian Institute of Technology Kanpur, Kanpur, India
10. Housing and Building National Research Center (2012) The Egyptian Code for Calculation of Loads and Forces on Civil Constructions and Building Works, ECP-201. Hous. Build. Natl. Res. Cent.
11. Housner GW (1963) The dynamic behavior of water tanks. Bull Seismol Soc Am 53:381–387. https://doi.org/10.1785/BSSA0530020381
12. Younan AH, Veletsos AS (1998) Dynamics of solid-containing tanks. I: Rigid tanks. J Struct Eng 124:52–61
13. Veletsos AS, Younan AH (1998) Dynamics of solid-containing tanks. II: Flexible tanks. J Struct Eng

124:62–70

14. Haroun MA, Housner GW (1981) Seismic design of liquid storage tanks. J Tech Counc ASCE 107:191–207. https://doi.org/10.1061/JTCAD9.0000080
15. Haroun MA, Ellaithy HM (1985) Seismically induced fluid forces on elevated tanks. J Tech Top Civ Eng 111:1–15. https://doi.org/10.1061/JTCEDL.0000023
16. Moslemi M, Kianoush MR, Pogorzelski W (2011) Seismic response of liquid-filled elevated tanks. Eng Struct 33:2074–2084. https://doi.org/10.1016/j.engstruct.2011.02.048
17. El Damatty AA, Saafan MS, Sweedan AMII (2005) Experimental study conducted on a liquid-filled combined conical tank model. Thin-Walled Struct 43:1398–1417. https://doi.org/10.1016/j.tws.2005.04.003
18. Dutta SC, Dutta S, Roy R (2009) Dynamic behavior of R/C elevated tanks with soil–structure interaction. Eng Struct 31:2617–2629
19. Kianoush MR, Ghaemmaghami AR (2011) The effect of earthquake frequency content on the seismic behavior of concrete rectangular liquid tanks using the finite element method incorporating soil–structure interaction. Eng Struct 33:2186–2200
20. Livaoğlu R, Doğangün A (2006) Simplified seismic analysis procedures for elevated tanks considering fluid–structure–soil interaction. J Fluids Struct 22:421–439
21. Hussein, Yousef (2001) Dynamic Response of Elevated Tanks Considering Water Structure Soil Interaction. Bull Fac Eng Assiut Univ Vol 29 No 1 61–70
22. Meng X, Li X, Xu X, et al (2019) Earthquake response of cylindrical storage tanks on an elastic soil. J Vib Eng Technol 7:433–444
23. Jogi P, Jayalekshmi BR (2022) Effect of Soil-Structure Interaction on the Seismic Response of Elevated Water Tank BT - Recent Advances in Earthquake Engineering. In: Kolathayar S, Chian SC (eds) Recent Advances in Earthquake Engineering. Springer Singapore, Singapore, pp 237–248
24. Al-Khafaji MS, Mohammed AS, Salman MA (2021) ANSYS-based structural analysis study of elevated spherical tank exposed to earthquake. Eng Technol J 39:870–883. https://doi.org/10.30684/etj.v39i6.460
25. Patel CN, Patel HS (2014) Seismic Response of RC Elevated Water Tank Considering Site Specific Acceleration Time History. In: Proceedings of International Conference on Advances in Tribology and Engineering Systems. Springer, pp 451–463
26. Abbood IS, Mahmod M, Hanoon AN, et al (2018) Seismic response analysis of linked twin tall buildings with structural coupling. Int J Civ Eng Technol 9:208-219.
27. Kumar D, Chiang C-H, Lin Y-C (2022) Experimental vibration analysis of large structures using 3D DIC technique with a novel calibration method. J Civ Struct Heal Monit 12:391–409. https://doi.org/10.1007/s13349-022-00549-5
28. Tatsumi A, Iijima K, Fujikubo M (2022) Estimation of still-water bending moment of ship hull girder using beam finite element model and ensemble Kalman filter. In: International Conference on Offshore Mechanics and Arctic Engineering. American Society of Mechanical Engineers, p V002T02A017
29. Zhang M, Schreier S, Hopman H (2020) Digital Image Correlation Application to a Modular Flexible Floating Structure. In: The 30th International Ocean and Polar Engineering Conference. International Society of Offshore and Polar Engineers (ISOPE)
30. Zhang P, Carretto A, Porfiri M (2020) Simultaneous digital image correlation/particle image velocimetry to unfold fluid–structure interaction during air-backed impact. J Fluids Struct 95:. https://doi.org/10.1016/j.jfluidstructs.2020.102980
31. Luo X, Zhang S, Li A, et al (2023) Steel rebar effect on tensile and cracking behavior of UHPFRC based on direct tensile tests and digital image correlation. Cem Concr Compos 137:. https://doi.org/10.1016/j.cemconcomp.2023.104940
32. Aryanto A, Revolis M, Oribe Y, Yo H (2023) Application of digital image correlation method in RC and FRC beams under bending test. Int J GEOMATE 24:118–125. https://doi.org/10.21660/2023.101.g12275

33. Bauer HF (1964) Fluid oscillations in the containers of a space vehicle and their influence upon stability. National Aeronautics and Space Administration, Washington, D.C., USA
34. Malhotra PK, Wenk T, Wieland M (2000) Simple procedure for seismic analysis of liquid-storage tanks. Struct Eng Int 10:197–201. https://doi.org/10.2749/101686600780481509
35. ACI Committee 371 (1998) Guide for the Analysis, Design, and Construction of Concrete-Pedestal Water Towers (ACI 371R-98). Farmington Hills, MI, USA
36. I. EH (1976) Seismic Design of Liquid-Storage Tanks. J Struct Div 102:1659–1673. https://doi.org/10.1061/JSDEAG.0004421
37. Livaoğlu R, Doğangün A (2006) Simplified seismic analysis procedures for elevated tanks considering fluid-structure-soil interaction. J Fluids Struct 22:421–439. https://doi.org/10.1016/j.jfluidstructs.2005.12.004
38. Chopra AK (2012) Dynamics of Structures: Theory and Applications to Earthquake Engineering (4th ed.). Pearson Education, Inc. (Prentice Hall)
39. Livaoğlu R, Doğangün A (2006) Evaluation of Seismic Models for Fluid-Elevated Tanks Systems Suggested in Codes. In: 7th International Congress on Advances in Civil Engineering. Istanbul, pp 1–10
40. Livaoglu R, Dogangun A (2005) Seismic evaluation of fluid-elevated tank-foundation/soil systems in frequency domain. Struct Eng Mech 21:101–119. https://doi.org/10.12989/sem.2005.21.1.101
41. Lubkowski ZA, Duan X (2001) EN1998 Eurocode 8: Design of structures for earthquake resistance. Proc Inst Civ Eng - Civ Eng 144:55–60. https://doi.org/10.1680/cien.2001.144.6.55
42. ACI Committee 350 (2006) Seismic Design of Liquid-containing Concrete Structures and Commentary (ACI 350.3-06). American Concrete Institute, Farmington Hills, MI, USA
43. Mori C, Sorace S, Terenzi G (2015) Seismic assessment and retrofit of two heritage-listed R/C elevated water storage tanks. Soil Dyn Earthq Eng 77:123–136. https://doi.org/10.1016/j.soildyn.2015.05.007
44. American Society of Civil Engineers (2017) Minimum Design Loads and Associated Criteria for Buildings and Other Structures. American Society of Civil Engineers, Reston, Virginia, USA
45. ANSYS Inc (2010) ANSYS Mechanical APDL, Release 13.0. Canonsburg, PA: ANSYS Inc.
46. Drosos JC, Tsinopoulos S V, Karabalis DL (2005) Seismic response of spherical liquid storage tanks with a dissipative bracing system. In: 5th GRACM International Congress on Computational Mechanics, Limassol. Patras, Greece, pp 313–319
47. Gregoriou VP, Tsinopoulos S V, Karabalis DL (2005) Seismic analysis of base isolated liquefied natural gas tanks. In: 5th GRACM International Congress on Computational Mechanics. Patras, Greece, pp 305–312
48. ZHAI X, WANG H, FAN F (2014) Multi-physics coupling method and applications of fluid-structure interaction on LNG storage tanks. In: 11th world congress on computational mechanics (WCCM XI), Barcelona, Spain. pp 1–11
49. Moslemi M (2011) Seismic response of ground cylindrical and elevated conical reinforced concrete tanks. Ryerson University
50. Buckingham E (1914) On Physically Similar Systems; Illustrations of the Use of Dimensional Equations. Phys Rev 4:345–376. https://doi.org/10.1103/PhysRev.4.345
51. Qin X, Chen Y, Chouw N (2013) Effect of uplift and soil nonlinearity on plastic hinge development and induced vibrations in structures. Adv Struct Eng 16:135–147. https://doi.org/10.1260/1369-4332.16.1.135
52. Omidinasab F, Shakib H (2012) Seismic response evaluation of the RC elevated water tank with fluid-structure interaction and earthquake ensemble. KSCE J Civ Eng 16:366–376. https://doi.org/10.1007/s12205-011-1104-1
53. Bozorgmehrnia S, Ranjbar MM, Madandoust R (2013) Seismic behavior evaluation of concrete elevated water tanks. Civ Eng infrastructures J 46:175–188
54. Shakib H, Omidinasab F, Ahmadi MT (2010) Seismic demand evaluation of elevated reinforced concrete water tanks. Int J Civ Eng 8:204–220

55. Shakib H, Omidinasab F (2011) Effect of earthquake characteristics on seismic performance of RC elevated water tanks considering fluid level within the vessels. Arab J Sci Eng 36:227–243. https://doi.org/10.1007/s13369-010-0029-1

56. Quadri SS, Sawant RM (2017) Seismic Behavior of RC Elevated Water Tank under the Impact of Liquid Sloshing. Recent Trends Civ Eng Technol 7:21–30

57. Shahana T, Deepu SP (2023) Seismic Vulnerability Assessment of Baffled Elevated Water Tank with Fluid–Structure–Soil Interaction Having Variable Staging Pattern BT - Proceedings of SECON'23. In: Nehdi M, Hung MK, Venkataramana K, et al (eds) International Conference on Structural Engineering and Construction Management. Springer, Cham, pp 667-676.doi.org/10.1007/978-3-031-39663–2_56